Received 1 February 2024; revised 18 February 2024; accepted 19 February 2024. Date of publication 21 February 2024; date of current version 4 March 2024.

Digital Object Identifier 10.1109/OJCOMS.2024.3368202

Precise Frequency Response of COTS LED for VLC Using Internal Quantum Efficiency Metric

JIAN XIONG [1,2], MENGHAN LI [2,3], RUNXIN ZHANG [2,3], LU LU [2,3] (Member, IEEE), QIFU TYLER SUN [1] (Member, IEEE), AND KEPING LONG [1] (Senior Member, IEEE)

[1]School of Computer and Communication Engineering, University of Science and Technology Beijing, Beijing 100094, China

[2]Key Laboratory of Space Utilization, Technology and Engineering Center for Space Utilization, Chinese Academy of Sciences, Beijing 100094, China

[3]School of Aeronautics and Astronautics, University of Chinese Academy of Sciences, Beijing 100049, China

CORRESPONDING AUTHOR: L. LU (e-mail: lulu@csu.ac.cn)

The work of Jian Xiong, Qifu Tyler Sun, and Keping Long was supported in part by the National Natural Science Foundation of China under Grant 62271044. The work of Menghan Li, Runxin Zhang, and Lu Lu was supported in part by the Key Research Program of the Chinese Academy of Sciences under Grant ZDRW-KT-2019-1-0103.

ABSTRACT Visible light communications (VLC) utilizing LEDs for transmissions have been widely considered a revolutionary solution for next-generation networks such as 6G. Frequency response (FR) is of great importance for LEDs, but the inherent internal quantum efficiency (IQE) of LEDs is often disregarded, resulting in imprecise FR models. Although it is widely known that IQE varies with the injected direct current (DC), the impact of IQE on the frequency response has not been thoroughly analyzed. To address this issue, we have developed a precise electro-optical (E-O) FR model by incorporating the ABC model of IQE, named IQE-FR. To validate the accuracy of IQE-FR, we conducted the experiments using commercial off-the-shelf (COTS) LEDs including a tri-color LED and three monochromatic LEDs. The IQE-FR model aligns well with the experimental findings in terms of the maximum FR value, while state-of-the-art FR models that ignore the IQE effects do not yield consistent results. Specifically, we discovered that the red LEDs exhibit a stable DC gain when the biasing current rises to 300 mA, but the highest DC gain for green and blue LEDs can only be achieved under 100 mA. For green and blue LEDs, the biasing currents are much lower than their typical working currents (350 mA and 500 mA). To address the trade-off between luminance and DC gain, we propose cascading multiple LEDs operating at a low current corresponding to the maximum response. Experimental results demonstrate that four cascaded monochromatic LEDs exhibit similar bandwidth and response gain larger than 11 dB compared to a single LED at the same biasing current while delivering four times the emission power, which is very close to the theoretical value of 12 dB. Furthermore, we find that the DC gain improvement by cascading multiple LEDs is nonlinear and bounded by an upper limit as the number of LEDs increases, and as a cost-effective solution, a few tens of LEDs is recommended. To the best of our knowledge, this is the first attempt to apply the IQE model to study the LEDs' precise FR performances for VLC. We believe that the precise IQE-FR model opens new avenues for optimizing VLC system performance by considering the effects of IQE.

INDEX TERMS Visible light communications, frequency response, internal quantum efficiency.

I. INTRODUCTION

THE RAPID advancement of information technology has resulted in a shortage of available electromagnetic spectrum bands. To meet the exponentially increasing demand for mobile data communication, visible light communications (VLC) has been identified as a promising technology for next-generation communication such as 6G, offering hundreds of terahertz of license-free bandwidth [1], [2], [3]. One pivotal element in the VLC system is the light source, encompassing devices like the laser diode (LD),

TABLE 1. Comparison of different LED models.

Papers, year	LED type	Low-pass frequency response model	Including equivalent circuit analysis	DC gain against biasing current	Application of LED's IQE effect
[5], 1975	Self-made	First-order	Yes	Not mentioned	Not mentioned
[6], 1976	Self-made	First-order	No	Not mentioned	Not mentioned
[7], 1998	Not mentioned	First-order	Yes	Not mentioned	Not mentioned
[8], 2017	Self-made	Second-order	Yes	Not mentioned	Not mentioned
[9], 2021	1.OSRAM LE-UW-S2WN 2.Cree XLamp XR-E 3.Luminus SST-90-W	Second-order	No	Not mentioned	Not mentioned
[10], 2021	1.Lumileds Luxeon Rebel 2.LXML-PWC2	>Second-order	Yes	Not mentioned	Not mentioned
[11], 2022	1.Cree CXB1830-0000-000N0BV265E 2.Cree XHP70A-01-0000-0D0BN40E1 3.OSRAM LZ4-40CW08-0065	>Second-order	Yes	Constant	Not mentioned
[12], 2024	OSRAM LE RTB N7WM	Second-order	Yes	Constant	Not mentioned
This work	1.OSRAM LE RTB N7WM 2.OSRAM OSLON SSL GR 3.OSRAM OSLON SSL GB 4.OSRAM OSLON SSL GT	Second-order	Yes	Nonlinear function of DC	ABC model of IQE

superluminescent diode (SLD), light-emitting diode (LED), and so on. Especially, solid-state LED devices are widely used due to their energy efficiency, durability, longevity, and design flexibility [4]. These attributes make LEDs an essential hardware basis for the implementation of VLC.

Some characteristics of LEDs are crucial for VLC systems, including frequency response (FR), optical power-current (P-I) characteristics, and voltage-current (V-I) characteristics. The study of the frequency response of LEDs dates back to the 1970s. In [5] and [6], the space-charge capacitance originating from the P-N junction of the LED and the electron lifetime in the carrier recombination process were found as two primary factors influencing the FR, and a first-order equivalent circuit considering diffusion and space-charge capacitance of the LED is given. The authors of [7] first measured the impedance of LED under different biasing currents, and then deduced the differential diode resistance, diffusion capacitance, and parasitic resistance of the first-order equivalent circuit based on the experimental data. In 2017, [8] investigated the impact of differential carrier lifetime and transport effects in electrically injected III-nitride LEDs, then developed a detailed second-order equivalent circuit model for LEDs, and finally validated its accuracy through experiments. The experimental results provided evidence for the correctness of the second-order equivalent circuit model. However, the derived frequency response does not consider the electro-optical (E-O) conversion efficiency. Reference [9] proposed a math model of frequency model with one zero and two poles but lacks an equivalent circuit which makes the lack of bandwidth calculation and DC gain. Reference [10] built a higher order equivalent circuit considering the influence of packeting and [11] proposed a high-order model suit for white LED based on the classical second-order model in [8], but these models treated the E-O conversion a constant without considering the influence of internal quantum efficiency (IQE). Reference [12] studied the equalizer of LED based on its second-order equivalent circuit and successfully designed a wide-band transmitter. The measured results in [12] and [13] show that as the biasing current increases and exceeds a threshold value, the magnitude of FR will decrease but the authors did not give an explanation. Table 1 presents a comparison of the literature above.

The P-I relationship is of particular importance and it is nonlinear due to the variation of IQE at different currents. The IQE of an LED reaches its peak, regardless of the emission wavelength, at current densities well below the operating current, and as the current increases, the IQE gradually decreases, exhibiting a phenomenon commonly known as "droop" [14]. From the mathematical expressions, the nonlinearity could be modeled as a memory-less nonlinear model (polynomial model) [15], and a memory nonlinear model (Wiener model) [16]. However, these approaches disregarded the physical mechanisms underlying the nonlinearity. The nonlinearity behavior of LEDs is primarily influenced by recombination and leakage in the active region [17]. Reference [18] proposed a more practical LED model based on the dynamic rate equation and the ABC model of IQE, which can accurately characterize the nonlinear effect of the static and transient behavior. Based on the nonlinear model, the authors of [19] designed and optimized the post-distorter. However, the literature above does not refer to the frequency response of LED.

The E-O frequency response, derived from the equivalent circuit and the P-I relationship, provides valuable information about gain and bandwidth and has garnered significant attention [20]. However, traditionally, the impact of IQE on the E-O frequency response has been overlooked or not thoroughly investigated [8], [21], [22], [23]. This letter argues that IQE, which varies with current density, can indeed influence the E-O frequency response, emphasizing the importance of selecting an appropriate quiescent operating point for VLC systems. Due to the significantly lower impedance of a turned-on LED compared to 50 Ohms, an impedance mismatch with the signal source can result in a high reflection coefficient. While adding a lumped element, such as a resistor, may lead to signal energy consumption and degradation of the modulation index, so cascading multiple LEDs with higher impedance can be advantageous.

In this paper, we first introduce the equivalent circuit and IQE model of an LED, based on which, we derive the E-O frequency response (FR) of the LED, named IQE-FR. We then validate the IQE-FR model using different types of LEDs using their corresponding parameters given in the datasheet. Finally, to further increase the luminance performance of the LED without sacrificing the maximum FR, we propose a method to cascade multiple LEDs by operating at a low current. The contributions of this paper are summarized as follows:

1) We present an IQE-FR model for LEDs, combining the ABC model of IQE with the second-order equivalent circuit model of LEDs, to study their precise frequency responses (FR). Different from the conventional understanding that IQE values are commonly assumed to be fixed terms in the VLC research literature, the IQE-FR model reveals, for the first time, that IQE values may greatly affect the magnitude of the FR while leaving the bandwidth changed.
2) We have built PCB boards and conducted experiments using four COTS LEDs to validate the preciseness of the proposed IQE-FR model. Experimental results agree with the analytical results derived from the IQE-FR model. Interestingly, two different red LED brands demonstrate a stable DC gain after they reach a peak value. However, the DC gains of both green and blue LEDs reach peak values at a lower current compared with their corresponding typical forward currents, and then decrease as their biasing currents increase. Our findings indicate that, compared with the red LED, the maximum DC gains of green and blue LEDs are achieved at the currents lower than typical forward currents, leading to suboptimal LED luminance performances, which may consequently reduce the coverage range or transmission distance of a VLC link.
3) To address the trade-off problem between LEDs' luminance and DC gains for blue and green LEDs, we propose to serially cascade multiple LEDs operating at a low current. Experimental results reveal that four cascaded monochromatic green (and blue) LEDs exhibit FR gain larger than 11 dB (close to the theoretical limit 12 dB) compared to a single LED at the same biasing current while having four times the emission power and the same bandwidth. Furthermore, we find that the DC gain improvement by cascading multiple LEDs of the same color in serial is nonlinear and bounded by an upper limit as the number of LEDs increases. As a cost-effective solution, a few tens of LEDs are recommended.

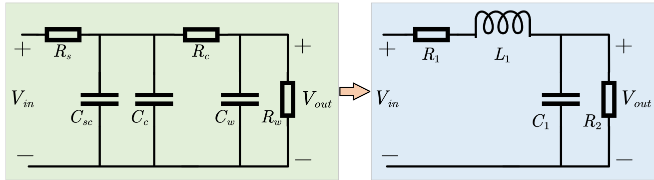

(a) (b)

FIGURE 1. (a) The small-signal intrinsic equivalent circuit of LED in [8], (b) the second-order equivalent circuit used in this paper.

II. THE SECOND-ORDER CIRCUIT MODEL OF LED

From [8], the equivalent circuit of LED is shown in Fig. 1 (a). The space charge capacitance C_{sc} is from the P-I-N junctions which means a small portion of the injected current must charge the capacitance C_{sc} to compensate for the built-in voltage of the P-I-N junctions. C_c is the capacitance associated with the unconfined carriers in the cladding region. C_w is defined as the capacitance associated with the confined carriers in the MQW (Multiple Quantum Well). $R_c = \frac{\tau_c}{C_c}$ and $R_w = \frac{\tau_{rec}}{C_w}$ represent the resistances due to carriers in the cladding and MQW regions, respectively. Carriers in the cladding region diffuse toward the MQW layers under a forward bias with a time delay of τ_{diff} and are captured by the QW with a capture rate of τ_{cap}. The total delay experienced by unconfined carriers in the cladding (N_c) region is defined as the cladding delay $\tau_c = \tau_{diff} + \tau_{cap}$. After capture by the QWs, the carrier population in the MQW (N_w) can be altered by two processes: recombination (radiative and non-radiative), with rate τ_{rec}, and thermionic emission to the cladding region, with rate τ_{esc}. Any effects of the transport of carriers between the quantum wells are folded into the carrier recombination lifetime. In a word, the C_{sc}, C_c, and R_c are the parasitic parameters, while C_c and R_c are the parameters from the differential carrier lifetime. Eq. (2) and Eq. (1) are the electrical frequency response of the LED and the total input impedance, respectively.

$$\frac{V_{out}(\omega)}{V_{in}(\omega)} = \frac{\frac{R_w}{R_s+R_c}}{\left[\begin{array}{c}(1+j\omega\tau_{rec})\left(1+j\omega\frac{R_s}{R_s+R_c}\tau_0\right)\\ +\frac{R_w}{R_s+R_c}(1+j\omega R_s C_{tot})\end{array}\right]}$$

$$\overset{R_sC_{tot}\approx 0}{\approx} \frac{R_w}{R_s+R_c+R_w}\cdot\frac{1}{\left[\begin{array}{c}(j\omega)^2\frac{R_s\tau_0\tau_{rec}}{R_s+R_c+R_w}+1\\+j\omega\frac{R_s\tau_0+\tau_{rec}(R_s+R_c)}{R_s+R_c+R_w}\end{array}\right]}, \quad (1)$$

$$Z_{in1}(\omega)=R_s+\frac{R_c(1+j\omega\tau_{rec})+R_w}{(1+j\omega\tau_{rec})(1+j\omega\tau_0)+j\omega C_{tot}R_w}, \quad (2)$$

where $C_{tot}=C_c+C_{sc}$ and $\tau_0=R_cC_{tot}=\tau_c+R_cC_{sc}$. τ_0 is referred to as the diode time constant (RC constant).

The LED frequency response $H_{LED}(\omega)$ could be simplified into another two types under low current density and high current density, which are denoted as

$$H_1(\omega)\approx\frac{\frac{R_w}{R_s+R_c+R_w}}{\left(1+j\omega\frac{R_s+R_c}{R_s+R_c+R_w}\tau_{rec}\right)}, \quad (3)$$

and

$$H_1(\omega)\approx\frac{\frac{R_w}{R_s+R_c}}{(1+j\omega\tau_{rec})\left(1+j\omega\frac{R_s}{R_s+R_c}\tau_0\right)}. \quad (4)$$

To be noticed, Eq. (3) and Eq. (4) can not be derived from Fig. 1 (a), directly. Therefore, the equivalent circuit is not perfectly compatible with two transfer functions. To eliminate this flaw, we propose converting the circuit into the other second-order circuit shown in Fig. 1 (b), and the frequency response is given by:

$$H_2(\omega)=\frac{R_2}{R_1+R_2}\frac{1}{(j\omega)^2\frac{L_1C_1R_2}{R_1+R_2}+j\omega\frac{L_1+C_1R_1R_2}{R_1+R_2}+1}, \quad (5)$$

and the input impedance is

$$Z_{in2}=R_1+j\omega L_1+\frac{R_2}{1+j\omega C_1R_2}. \quad (6)$$

Comparing two expressions of frequency response $H_1(\omega)$ and $H_2(\omega)$, we can see that they are the second-order low-pass function, which means that two equivalent circuits in Fig. 1 could be converted. Let $R_1=R_s+R_c$, $L_1=R_s\tau_0=R_sR_c(C_sc+C_c)$, $C_1=C_w$, and $R_2=R_w$, we can make $H_1(\omega)=H_2(\omega)$. When considering the signal source output impedance R_o in a practical circuit, the frequency response function is written by

$$H_{\text{LED}}(\omega)=\frac{K_e}{(j\omega)^2\frac{L_1C_1R_2}{R_1+R_2+R_o}+j\omega\frac{L_1+C_1R_2(R_1+R_o)}{R_1+R_2+R_o}+1}, \quad (7)$$

where $K_e=\frac{R_2}{R_1+R_2+R_o}$. Back to Fig. 1 (a), R_w+R_c equals the differential diode resistance R_d which can be derived from the V-I characteristic of a diode which is described by Shockley's equation for the forward and reverse-bias regions [24]:

$$I_d=I_s\left(e^{\frac{V_d}{nV_T}}-1\right), \quad (8)$$

where I_s is the reverse saturation current; V_d is the applied forward-bias voltage across the diode; $1\le n\le 2$ is an ideality factor, which is a function of the operating conditions, physical construction, and a wide variety of factors. The voltage V_T in Eq. (8) is called the thermal voltage and is determined by

$$V_T=\frac{kT}{q}, \quad (9)$$

where $k=1.38\times10^{-23}$ J/K is Boltzmann's constant; T is the absolute temperature in kelvins; $q=1.60217663\times10^{-19}$ C is the elementary charge. Solving (8) for V_d and differentiating V_d with respect to I_d, we can get the expression of the expression of R_d:

$$R_d=\frac{\partial V_d}{\partial I_d}=nV_T\frac{1}{I_d+I_s}. \quad (10)$$

According to Eq. (10), R_d is inversely proportional to I_d. Since the output impendence of the signal source R_o is usually 50 Ω, and R_d is about a few tenths of an Ohm [25], so R_2 is far smaller than R_1+R_o, and the frequency response $H_{LED}(\omega)$ can be converted into a more simple type:

$$H_{LED}(\omega)\overset{R_2\ll R_1+R_o}{\approx}\frac{R_2}{R_1+R_o}\frac{1}{[j\omega C_1R_2+1]\left[j\omega\frac{L_1}{R_1+R_o}+1\right]}. \quad (11)$$

It is clear that Eq. (11) is similar to Eq. (4), except for the additional impedance from the signal source. The $\frac{1}{C_1R_2}$ and $\frac{R_1+R_o}{L_1}$ still represent the carrier recombination lifetimes and RC time constant, respectively. The carrier recombination process dominates the frequency response in the small area LED, as the enlarging of the PN junction, the RC characteristic gradually plays an important role in the frequency response. Generally, the RC time constant is smaller than the carrier recombination lifetimes, which means that $\omega_\tau=\frac{1}{C_1R_2}<\omega_{rc}=\frac{R_1+R_o}{L_1}$. When two angular frequencies are distinct and have big differences, the 3dB bandwidth of LED is only decided by ω_τ. In [20], the bandwidth is inversely proportional to the carrier lifetime $\tau_{rec}=\sqrt{\frac{K_n}{I_d}}$, where K_n is a proper constant. Therefore, the bandwidth is

$$W_\tau=\frac{1}{2\pi}\sqrt{\frac{I_d}{K_n}}, \quad (12)$$

where K_n is a constant. When it is necessary to consider the RC constant in high-power LED, the bandwidth can be written as

$$W=\frac{1}{2\pi\sqrt{\tau_{rec}^2+\tau_0^2}}. \quad (13)$$

III. THE HIGH-GAIN TRANSMITTER DESIGN BASED ON E-O FREQUENCY RESPONSE MODEL USING IQE

An LED can be simply treated as a resistor once it is turned on and it can generate photons when the current passes through it. From [26], the emission power or flux of a LED is generally considered to be linearly related to the input current I_i, which is written as:

$$\Phi=\eta_{le}\eta_{int}\frac{hc}{q\lambda}I_i, \quad (14)$$

where $h = 6.626 \times 10^{-34}$ J · s is the Planck's constant; $q = 1.60217663 \times 10^{-19}$ C is the elementary charge; c is the velocity of light in the vacuum; λ is the dominated wavelength; η_{le} is the light extraction efficiency from the chip and η_{int} is the internal quantum efficiency. In most literature about VLC, η_{int} is assumed to be constant, so a stable linear relationship is built between optical power and driving current. In fact, η_{int} is influenced by the current, especially in high-current LED [14]. The IQE is usually represented by the ABC model [27]:

$$\eta_{int}(N) = \frac{BN^2}{AN + BN^2 + CN^3}, \tag{15}$$

where A, B, and C coefficients represent Shockley–Read–Hall (SRH) nonradiative recombination, bimolecular radiative recombination, and Auger recombination, respectively. N is carrier density in the device's active region. The optimum IQE is obtained by setting $\frac{d\eta_{int}(N)}{dN} = 0$ and the corresponding carrier density is given by

$$N_p = \sqrt{\frac{A}{C}}. \tag{16}$$

The N is related to the injection current I_i [28]:

$$I_i = qSW_{\mathrm{QD}}\left(AN + BN^2 + CN^3\right), \tag{17}$$

where S is the cross-sectional area of the LED; I_i is the injection current; W_{QD} represents the total thickness of approximately 25 to 30 nm of the quantum dot active region. $S \cdot W_{QD}$ is the volume of the active region with intensive carrier recombination.

The optimal injecting current can be computed by bringing Eq. (16) into Eq. (18). The expression of N with respect to J is complex and we can refer to [29] which is given by:

$$N(I_i) = \frac{-B + \sqrt{D}\left(\kappa(I_i) + \frac{1}{\kappa(I_i)}\right)}{3C}, \tag{18}$$

where

$$\kappa = \sqrt[3]{\chi + \sqrt{\chi^2 - 1}}, \tag{19}$$

$$\chi = \frac{9ABC - 2B^3 - 27C^2 d}{2\left(\sqrt{D}\right)^3}, \tag{20}$$

$$D = B^2 - 3AC, \tag{21}$$

$$d = -\frac{I_i}{qSW_{\mathrm{QD}}}. \tag{22}$$

Bringing Eq. (18) into Eq. (15), we can also get the relationship between IQE and injecting current.

From the equivalent circuit of LED, we know only the current passing through the R_w could generate the photons. We define the AC signal passing through the R_w as I_s, so under a biasing current I_d, the total injection current passing through the R_w is $I_i = I_d + I_s$. We temporarily neglect the influence of I_d on calculating the frequency response of the LED, so we can remove it in calculating the E-O frequency response. Given the voltage of AC signal V_s, we can get the expression of I_s from Eq. (11) and Ohm's law:

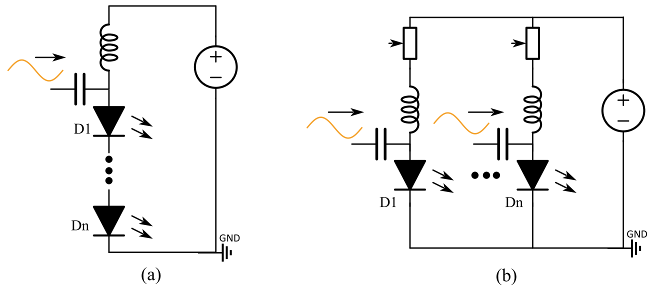

FIGURE 2. **(a) Cascading LEDs in serial, (b) cascading LEDs in parallel.**

$$I_s = \frac{V_s H_{LED}(\omega)}{R_w} = \frac{V_s}{R_1 + R_o}\frac{1}{(j\omega_\tau + 1)(j\omega_{rc} + 1)}. \tag{23}$$

Bring Eq. (23) into Eq. (14), we can get the E-O response function:

$$\begin{aligned} H_{EO}(\omega) &= \frac{\Phi_o}{V_s} \\ &= \eta_{le}\eta_{int}(I_d)\frac{hc}{q\lambda}\frac{1}{R_1 + R_o}\frac{1}{(j\omega_\tau + 1)(j\omega_{rc} + 1)} \\ &\triangleq K_{EO}\frac{1}{(j\omega_\tau + 1)(j\omega_{rc} + 1)}, \end{aligned} \tag{24}$$

where the $K_{EO} = \eta_{le}\eta_{int}(I_d)\frac{hc}{q\lambda}\frac{1}{R_1+R_o}$ is called the DC gain because $K_{EO} = H_{EO}(0)$. The η_{int} can be as high as 90% and the η_{le} is usually $> 75\%$. If considering the loss caused by the electrical contacts and series resistances, the minimum overall efficiency could be below 50%. $\frac{hc}{q\lambda} \approx 2$ for 635 nm light, but the maximum of $\frac{1}{R_1+R_o}$ is smaller than 0.02. Therefore, the maximum loss in the modulation is decided by the differential diode resistor of the LED and the output impedance of the signal source. We assume that the IQE η_{int} and differential diode resistance R_d are only influenced by the DC signal I_d, which is reasonable in circuit analysis [24].

We know that the droop phenomenon may degrade the IQE of LED, so improving the emission power of LED by increasing the biasing current can not improve the DC gain of LED. Therefore, to design a high-gain transmitter, we can cascade multiple LEDs and adjust the basing current to achieve the highest IQE. Although the emission power of a single LED is low, the total emission power of the transmitter can be high. The cascading could be common in the illumination for higher luminance, but the purpose is different in this paper. There are two ways to cascade LEDs, one in parallel and the other way in serial, which are shown in Fig. 2. In the serial cascading scenario, all LEDs are driven by the same current, and hence could only be modulated by the same AC signal. In the parallel configuration, an additional resistor is needed because very tiny differences in the internal resistances of the LEDs may lead to a high current passing through some LEDs, causing them to be destroyed. In the parallel setup, each LED's driving current can be independently adjusted using different resistors, allowing for different modulations on different LEDs.

The impedance of cascaded LEDs in serial is

$$Z_n = nR_1 + j\omega nL_1 + \frac{nR_2}{1 + j\omega C_1 R_2}, \tag{25}$$

where n is the number of LEDs. It can be found that the τ_{rec} of cascaded LEDs is unchanged, but the RC constant time τ_{rc} is multiplied. Therefore, as the number of LEDs increases, the RC effects could be a bottleneck of bandwidth. From $\omega_{rc} = \frac{R_1}{L_1} + \frac{R_o}{nL_1}$, we know that as n increases, the angular frequency ω_{rc} decreases and tends to a constant. As for small-area LEDs, the $\frac{R_1}{L_1} > \frac{1}{C_1 R_2}$, so the cascading of multiple LEDs doesn't influence the bandwidth. However, as for high-power LEDs with large areas, the situation may be different. Let I_η denote the biasing current corresponding to the highest IQE. From Eq. (14), the average emission power of cascaded LEDs is

$$\Phi_{o,m} = n\eta_{le}\eta_{int}(I_\eta)\frac{hc}{q\lambda}I_\eta, \tag{26}$$

and the responsivity of the transmitter based on cascaded LEDs is

$$K_{EO,n} = n\eta_{le}\eta_{int}(I_\eta)\frac{hc}{q\lambda}\frac{1}{nR_1 + R_o}. \tag{27}$$

Cascading multiple LEDs can significantly enhance the maximum response $K_{EO,n}$, but the increase is not proportional to the number of LEDs used due to the decrease of $\frac{1}{nR_1+R_o}$. As $n \to \infty$,$K_{EO,n}$ turns into

$$K_{EO,\infty} = \eta_{le}\eta_{int}(I_\eta)\frac{hc}{q\lambda}\frac{1}{R_1}. \tag{28}$$

For the sake of simplicity in comparison, we define the gain of $K_{EO,n}$ compared to K_{EO} as follows:

$$G_{DC,n} = \frac{K_{EO,n}}{K_{EO}} = \frac{n(R_1 + R_o)}{nR_1 + R_o} = \frac{R_1 + R_o}{R_1 + R_o/n}. \tag{29}$$

As $n \to \infty$, $G_{DC,n}$ turns into

$$G_{DC,\infty} = 1 + \frac{R_o}{R_1}, \tag{30}$$

so as the number of cascaded LEDs increases, the gain $G_{DC,n}$ tends to be a constant. For example, let $R_1 = 1$ Ω, $R_o = 50$ Ω, the $G_{DC,n}$ varying with n can be shown in Fig. 3. The max value of $G_{DC,\infty}$ is approximately 17 dB. The influence of η_{int} on cascaded LEDs is the same as the single LED, i.e., their P-I characteristics are the same. From the equivalent of LED, we can calculate the reflection coefficient [30]:

$$\Gamma(\omega) = \frac{R_1 + j\omega L_1 + \frac{R_2}{1+j\omega C_1 R_2} - R_o}{R_1 + j\omega L_1 + \frac{R_2}{1+j\omega C_1 R_2} + R_o}. \tag{31}$$

When $\omega = 0$, we get $\Gamma(0) = \frac{R_1+R_2-R_o}{R_1+R_2+R_o}$ that represents the DC reflection coefficient. Usually, the output impedance is 50 Ω, and $R_1 + R_2$ is equal to the differential diode resistance R_d which is far smaller than 50 Ω when the LED is turned on. Therefore, the reflection coefficient is high and then results in a high Voltage Standing Wave Ratio (VSWR). High VSWR can lead to signal attenuation and distortion and the situation should be avoided, so we need additional components to increase the impedance of the load. Cascading multiple LEDs may be a proper solution. On the one hand, it can reduce the reflection coefficient; on the other hand, it can improve the overall emission power, especially since the high biasing current is against the high responsivity of LED.

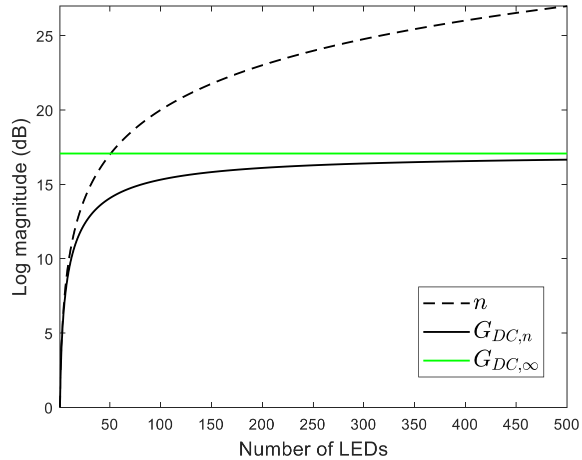

FIGURE 3. The gain of K_{EO} varied with the number of cascaded LEDs.

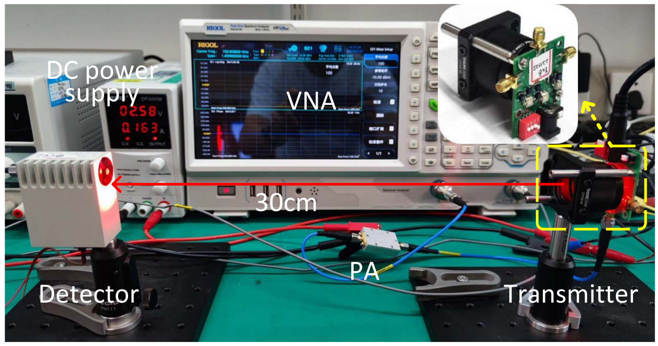

FIGURE 4. The experimental setup for measuring the frequency response of LED.

IV. EXPERIMENTAL RESULTS AND CONCLUSION

The experimental setup, depicted in Figure 4, comprises four LEDs: OSTAR LE RTB N7, OSLON SSL GR CS8PM1.23, OSLON SSL GB CS8PM1.13, and OSLON SSL GT CS8PM1.13 from OSRAM. The first LED is a tri-color LED consisting of three monochromatic LEDs, while the others are monochromatic LEDs. For the sake of simplicity, we refer to the first LED as OSTAR LED and the others as OSLON red LED, OSLON green LED, and OSLON blue LED. We designed the driver board in-house and used the following detectors: Hamamatsu C5658, MenloSystems FPD610-FS-VIS, and Thorlabs PDA10A2. Table 2 and Table 3 provide the main parameters of the LEDs and detectors. Notably, the OSLON series LEDs

TABLE 2. The main parameters of adopted LEDs.

Model		Dominant wavelength	Spectral bandwidth	Viewing angle	Max forward current	Length of light emitting area
OSTAR LE RTB N7WM	Red	617 nm	18 nm	120°	500mA	0.65mm
	Green	530 nm	35 nm	120°	500mA	0.65mm
	Blue	465 nm	18 nm	120°	500mA	0.65mm
OSLON SSL	Red	623.0 nm	16.0 nm	80°	1000mA	1mm
	Green	528.0 nm	30.0 nm	80°	1000mA	1mm
	Blue	470.0 nm	25.0 nm	80°	1000mA	1mm

TABLE 3. The main parameters of adopted detectors.

Model	Wavelength range	Bandwidth	Maximum responsivity	Detector active area diameter
Hamamatsu C5658	400 to 1000 nm	50kHz to 1GHz	50 A/W, M = 100	0.5mm
MenloSystems FPD610-FS-VIS	400 to 1000 nm	DC to 600 MHz	$2\times10^6 V_{pp}/W$	0.4 mm
Thorlabs PDA10A2	200 to 1100 nm	DC to 150 MHz	0.44 A/W	1 mm

have higher forward current and emission power than the OSTAR series. In the measurement setup, the Vector Network Analyzer (VNA) output signal is sent into a 5dB attenuator before being amplified by a power amplifier (PA) to enhance the electrical signal power. This amplified electrical signal is then utilized to modulate the optical signal in the transmitter. The transmission distance between the transmitter and detector is 0.2 M. On the receiver side, the optical signal is converted back into an electrical signal and transmitted to the VNA for analysis. The E-O frequency response could be measured by setting the photodetector as a far wider bandwidth than the LED. All measured results can be acquired from the link in the footnote.[1]

The maximum value of the measured frequency response is compared between four cascaded OSLON LEDs and a single LED. To ensure a fair comparison, the four LEDs are positioned closely together on the PCB, effectively treating them as a single entity during the measurement. As a result, the received optical power is four times that of a single LED, allowing for accurate and fair comparison and analysis. We cascaded multiple LEDs in serial for three reasons. First, it simplifies the circuit design, making it more straightforward to implement. Second, we do not need multiple AC signal inputs, temporarily. Last but not least, connecting the LEDs in series increases overall impedance, which offers the advantage of reducing the reflection coefficient.

We collected V-I and P-I data for three LEDs from their product datasheets [31]. The corresponding data were extracted from the figures on pages 9 and 10 using WebPlotDigitizer. Fig. 5 (a) shows the different V-I curves of the OSTAR LEDs from the measurement and Shockley's equation. It is clear that the measured data from [31] coincides with Shockley's equation. Figure 5 (b) illustrates the P-I curves, which represent the relationship between

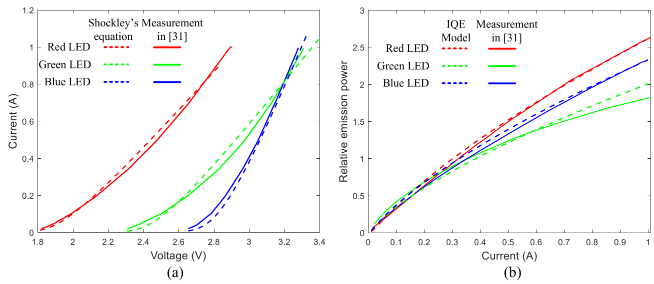

FIGURE 5. (a) The V-I curves of the OSTAR LEDs from the datasheet and Shockley's equation, (b) the P-I curves of OSTAR LEDs from the datasheet and IQE model.

emission power and current. The relative power value is the ratio of the emission power to its value at 350 mA. It is evident that the slopes of the curves gradually decrease, indicating that the optical emission power is not linearly related to the injection current. The green LED has the most obvious nonlinearity while the red LED demonstrates the weakest nonlinearity.

Fig. 6 (a) shows the S11 parameters of OSTAR LEDs. The S11 and S21 parameters are part of the scattering parameters of a two-port network, which consists of four parameters in total: S11, S12, S21, and S22. The average return loss of the unmatched red, green, and blue components of the OSTAR LED: −0.49 dB, −0.85 dB, and −0.79 dB, respectively. Such a high reflection coefficient will influence the S21 parameter of LED which can be shown in Fig. 6 (b). The frequency response curves fluctuate singularly and don't coincide with the IQE-FR model. After cascading a 47 Ω resistor in front of the LED, the return loss greatly degrades, with the highest value being less than −8 dB at 600 MHz. The measured frequency responses align with the proposed second-order frequency response model in Eq. (25). The parameters R_2, C_1, and L_1 are set to 0.5 Ω, 26 nF, and 24.48 nH, respectively. The OSTAR LED was measured at a constant biasing current of 150 mA using the Hamamatsu

[1]https://github.com/xiongxiongjian/The-measured-frequency-response-of-LED.

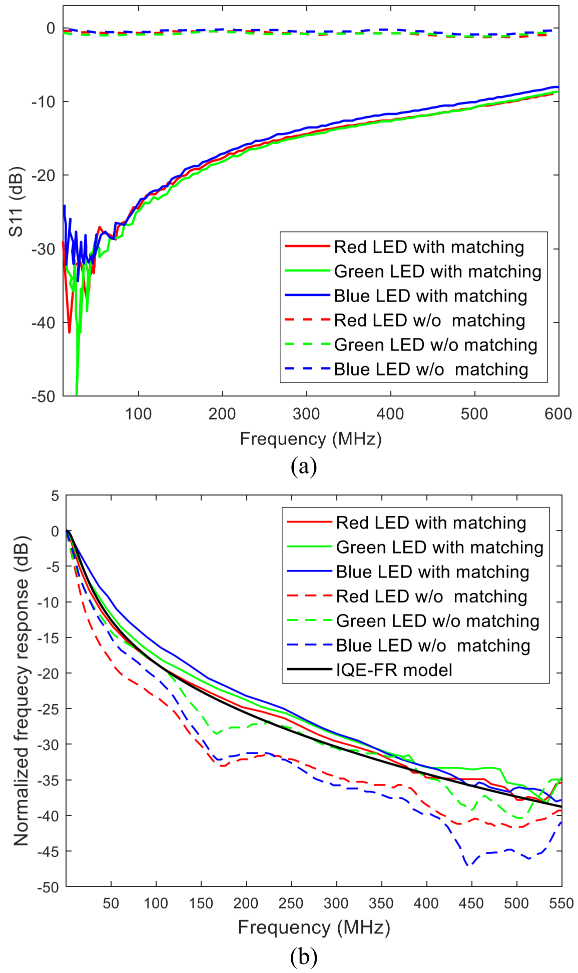

FIGURE 6. **(a) The S11 parameters of OSTAR LEDs with and without matching, (b) the measured E-O frequency responses of OSTAR LEDs and the simulation result of IQE-FR model.**

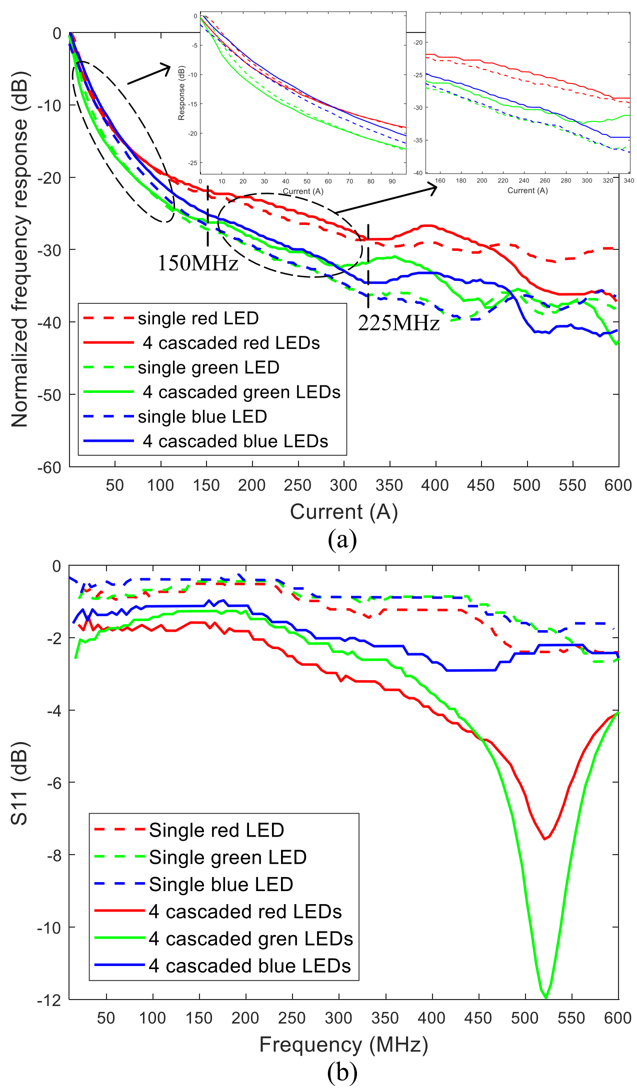

FIGURE 7. **(a) The normalized frequency response of the red, green, and blue LEDs from OSLON, (b) the corresponding S11 parameters of the red, green, and blue LEDs with and without matching.**

C5658 detector module with a 1GHz bandwidth as the receiver. Fig. 7 (b) illustrates the frequency responses of both single and cascaded OSLON LEDs. The frequency responses of the cascaded and single LEDs are similar within 150 MHz. However, the difference increases between 150 MHz and 225 MHz, eventually becoming distinguishable beyond 225 MHz. The cascaded LEDs exhibit higher impedance, which is beneficial in reducing the return loss. This can be observed in Fig. 7 (b).

Specifically, in white LEDs, the afterglow of the phosphors can affect the frequency response, making the measured result deviate from the model, as shown in Fig. 8. The white LED is OSRAM LUW CN7N and the measured data comes from [32]. The blue LED is OSLON SSL GT CS8PM1.13 which is adopted in this paper. We can see that the measured result of the white LED deviated from the model with about 150 MHz, but the situation did not occur on the blue LED. After adding a blue filter in front of the PD, we can eliminate the most yellow light generated from the phosphors and the measured frequency response model coincides with the frequency model much better. The frequency response of the phosphors can be modeled separately which is studied by [11].

Measuring the absolute value of η_{int} can be challenging, but we can obtain the normalized value $\eta_{int}/\max(\eta_{int})$, which reflects the variation trend of η_{int}. By calculating the slope of the P-I curve and normalizing it with respect to its maximum value, we can obtain the results shown in Fig. 9 (a). We can see that the slope curves of the red and blue LEDs from the data sheet [31] conform to the $\eta_{int}/\max(\eta_{int})$ from the ABC model described in Eq. (14). The parameters in their ABC models are listed in Table 4. Based on Eq. (25), both R_1 and η_{int} could influence the magnitude of the E-O frequency response. The R_d quickly decreases to a far smaller value than R_g when the LED is turned on so that the K_o is mainly decided by the η_{int}. We measured and calculated the maximum response of four LEDs under different biasing currents, as shown in Fig. 9

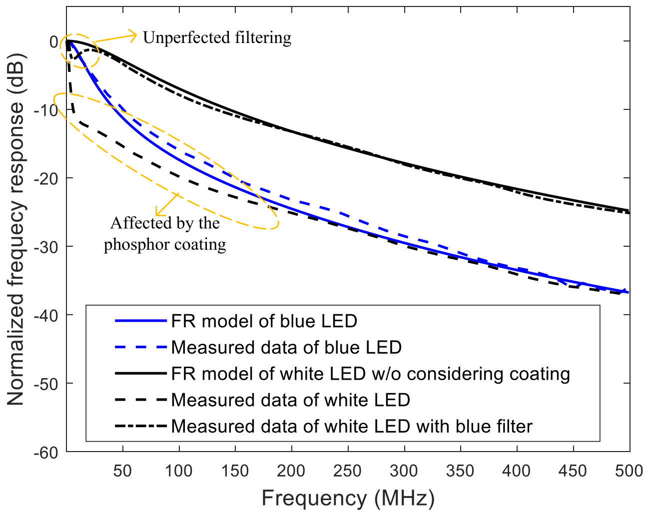

FIGURE 8. The frequency responses of blue LED, white LED with/without a blue filter, and the corresponding models.

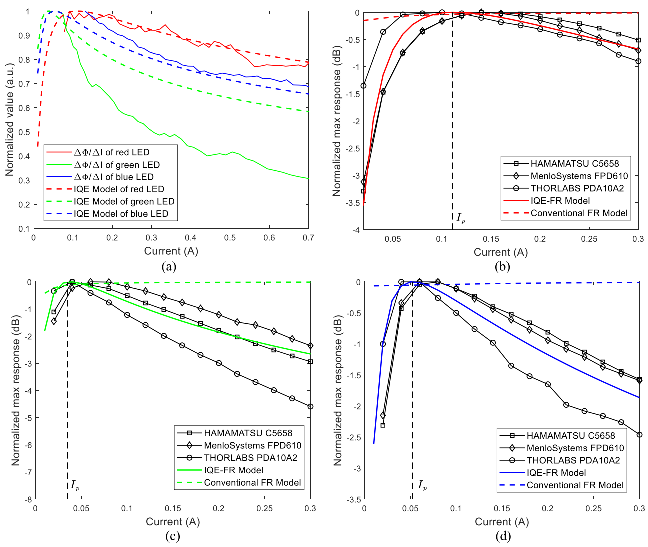

FIGURE 9. (a) The normalized value of the slopes of the P-I curves from OSTAR LEDs and the corresponding normalized η_{int}, (b)-(d) the normalized max frequency response of the red, green, and blue LED at different biasing currents and their corresponding theoretical results from the IQE-FR model. The results are measured using three different detectors: HAMAMATSU C5658, MenloSystems FPD610-FS-VIS, and THORLABS PDA10A2.

TABLE 4. The parameters in the ABC model of three LEDs.

LED		$\mathbf{A}(s^{-1})$	$\mathbf{B}(cm^3/s)$	$\mathbf{C}(cm^6/s)$
OSTAR	Red	9×10^7	3×10^{-10}	3.6×10^{-27}
	Green	2.81×10^8	6.4×10^{-9}	9.8×10^{-25}
	Blue	3.38×10^8	8.2×10^{-9}	8.3×10^{-25}
OSLON	Red	2.7×10^7	5×10^{-10}	3×10^{-28}
	Green	1.6×10^8	1.6×10^{-9}	7.5×10^{-26}
	Blue	1.04×10^8	1.3×10^{-9}	2.23×10^{-26}

(b), (c), (d) and Fig. 10 (b), (c), (d). The maximum response in the measurement is obtained at 100KHz and it means the power gain. The K_{EO} represents the voltage gain in

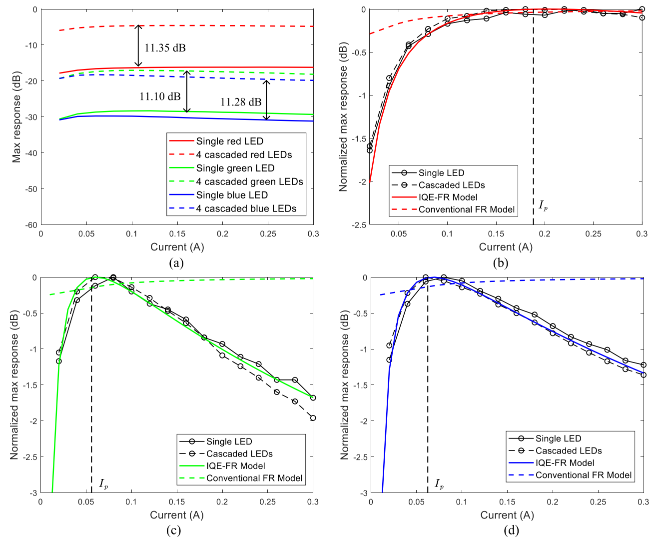

FIGURE 10. (a) The max response value of the single and cascaded LEDs, (b)-(d) the normalized max frequency response of the red, green, and blue LED at different biasing currents and their corresponding theoretical results from the IQE-FR model. The data are measured using Menlo Systems FPD610-FS-VIS.

the IQE-FR model. We have unified the units in their Log magnitude for fair comparison. To avoid detector saturation, we did not use any condenser lens to collimate the light on the transmitter side and collect the light on the receiver side. The experimental results show that the maximum frequency response of the red LED from OSTAR is obtained below 150 mA, while the other two LEDs reach the maximum value below 100 mA. The red LED from OSTLON is obtained below 250 mA, while the other two LEDs reach the maximum value below 100 mA. The maximum gain of the E-O frequency response for these LEDs is dependent on the biasing current I_d. This relationship aligns with the IQE-FR, rather than the conventional FR model [10], [11]. The theoretical optimal current I_p corresponding to the maximum value of DC gain is marked in Fig. 9 (b), (c), (d) and Fig. 10 (b), (c), (d). The variation of the max response values of three LEDs from OSLON is similar to the LED from OSTAR. The biasing current that makes them achieve the highest max frequency is smaller than the typical forward current, especially for the green and blue LEDs. After cascading four LEDs, the variation of max response values has no obvious difference with a single LED. The measurement circumstances of single and cascaded LEDs are the same, so we can compare their absolute magnitude which is shown in Fig. 10 (a). At the same biasing current, the cascaded red LEDs are on average 11.35 dB higher than the single LED, and the other two cascaded LEDs are at least 11.0 dB higher than the corresponding single LED. Theoretically, the power gain of the cascaded LEDs, operating at the same biasing current, should be 12 dB due to four times LEDs. The difference may be caused by the decrease of modulation current due to the increased impedance of cascaded LEDs which can be explained in

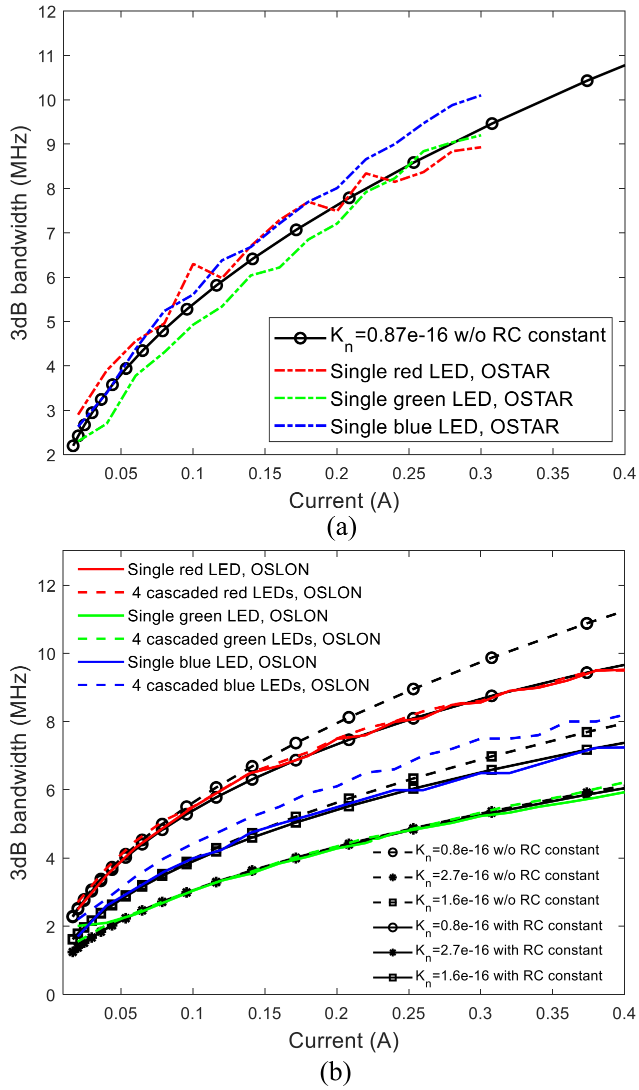

FIGURE 11. (a) The 3 dB bandwidth of the single LED OSTAR, (b) the 3 dB bandwidths of the single and cascaded OSLON LEDs.

Eq. (27). The 3 dB bandwidth of different LEDs varies with the biasing current can be shown in Fig. 11. The RC time constant τ_0 in OSTAR LED is far smaller recombination time τ_{rec}, so Eq. (12) could finely describe the bandwidth variation versus biasing current. In the OSLON LEDs, their bandwidth variations versus biasing current are different. Especially in the red LED, its bandwidth differs from the theoretical value of Eq. (12) as the biasing current increases but coincides with the theoretical value of Eq. (13) which indicates that the RC time constant τ_0 can't be overlooked. The three LEDs from OSTAR own a similar bandwidth but the three LEDs from OSLON are various. In Fig. 11 (b), the cascaded LEDs have almost the same bandwidth as a single LED from the same series which proves that the derived impedance of cascaded LEDs in Eq. (25) is correct and reveals that the differential recombination lifetime domains the bandwidth when the biasing current is not high.

To sum up, implementing cascading schemes can enhance the emission power, thereby increasing the transmission distance, coverage area, and SNR in VLC. A study by [33] experimentally demonstrates a VLC system that employs four cascaded LEDs to improve the SNR. Additionally, [34] proposes a scheme that utilizes multiple LEDs to cover a larger area. Furthermore, [35] introduces an optical spatial modulation technique employing multiple LEDs cascaded in parallel. However, these papers do not deeply study the physical characteristics of cascaded LEDs. In our work, we deeply studied the DC gain and bandwidth of four cascaded LEDs and found that the DC gain of cascaded LEDs is higher than a single LED, which is beneficial for improving the SNR. However, the improvement will gradually reach a limit as the LED number increases. The 3 dB bandwidth of cascaded LEDs is almost the same as the single LED because the carrier recombination time of each LED is not changed. However, the RC constant of cascaded LEDs is increased, and this will influence the part of frequency response in high frequency.

V. CONCLUSION

In this paper, we begin by presenting a simplified version of the equivalent circuit for COTS LEDs, based on [8]. Then we investigate the impact of the internal quantum efficiency (IQE) variation with biasing current and introduce a new frequency response model called IQE-FR, which incorporates the ABC model of IQE. To validate the accuracy of IQE-FR, we conduct the experiments using commercial off- the-shelf (COTS) LEDs including a tri-color LED and three monochromatic LEDs. The IQE-FR model aligns well with the experimental findings in terms of the maximum FR value, while state-of-the-art FR models that ignore the IQE effects do not yield consistent results. Finally, we cascade multiple LEDs in serial operating at a low current to enhance both luminance and DC gain, while simultaneously decreasing the return loss. The experimental results confirm that the cascading scheme successfully improves the DC gain by more than 11 dB without affecting the bandwidth. We also find that the DC gain improvement by cascading multiple LEDs is nonlinear and bounded by an upper limit as the number of LEDs increases, and as a cost-effective solution, a few tens of LEDs is recommended.

REFERENCES

[1] E. C. Strinati et al., "6G: The next frontier: From holographic messaging to artificial intelligence using subterahertz and visible light communication," *IEEE Veh. Technol. Mag.*, vol. 14, no. 3, pp. 42–50, Sep. 2019.
[2] L. E. M. Matheus, A. B. Vieira, L. F. Vieira, M. A. Vieira, and O. Gnawali, "Visible light communication: Concepts, applications and challenges," *IEEE Commun. Surveys Tuts.*, vol. 21, no. 4, pp. 3204–3237, 4th Quart., 2019.
[3] S. Aboagye, A. R. Ndjiongue, T. M. Ngatched, O. A. Dobre, and H. V. Poor, "RIS-assisted visible light communication systems: A tutorial," *IEEE Commun. Surveys Tuts.*, vol. 25, no. 1, pp. 251–288, 1st Quart., 2023.
[4] E. F. Schubert, *Light-Emitting Diodes*. Troy, NY, USA: E. Fred Schubert, 2018.

[5] T. P. Lee, "Effect of junction capacitance on the rise time of LED's and on the turn-on delay of injection lasers," *Bell Syst. Tech. J.*, vol. 54, no. 1, pp. 53–68, 1975.

[6] W. Harth, W. Huber, and J. Heinen, "Frequency response of GaAlAs light-emitting diodes," *IEEE Trans. Electron Devices*, vol. 23, no. 4, pp. 478–480, Apr. 1976.

[7] W. Cheung, P. Edwards, and G. French, "Determination of LED equivalent circuits using network analyser measurements," in *Proc. Conf. Optoelectron. Microelectron. Mater. Devices*, 1998, pp. 232–235.

[8] A. Rashidi et al., "Differential carrier lifetime and transport effects in electrically injected III-nitride light-emitting diodes," *J. Appl. Phys.*, vol. 122, no. 3, 2017, Art. no. 035706.

[9] R. Kisacik, M. Yagan, M. Uysal, A. Pusane, and A. Yalcinkaya, "A new LED response model and its application to pre-equalization in VLC systems," *IEEE Photon. Technol. Lett.*, vol. 33, no. 17, pp. 955–958, Sep. 1, 2021.

[10] X. Li, Z. Ghassemlooy, S. Zvanovec, and L. N. Alves, "An equivalent circuit model of a commercial LED with an ESD protection component for VLC," *IEEE Photon. Technol. Lett.*, vol. 33, no. 15, pp. 777–779, Aug. 1, 2021.

[11] P. Salvador, J. Valls, J. L. Corral, V. Almenar, and M. J. Canet, "Linear response modeling of high luminous flux phosphor-coated white LEDs for VLC," *J. Lightw. Technol.*, vol. 40, no. 12, pp. 3761–3767, Jun. 15, 2022.

[12] R. Zhang, J. Xiong, M. Li, and L. Lu, "Design and implementation of low-complexity pre-equalizer for 1.5 GHz VLC system," *IEEE Photon. J.*, vol. 16, no. 1, pp. 1–10, Feb. 2024.

[13] A. Rashidi, M. Monavarian, A. Aragon, A. Rishinaramangalam, and D. Feezell, "Nonpolar *m*-plane InGaN/GaN micro-scale light-emitting diode with 1.5 GHz modulation bandwidth," *IEEE Electron Device Lett.*, vol. 39, no. 4, pp. 520–523, Apr. 2018.

[14] A. Laubsch, M. Sabathil, J. Baur, M. Peter, and B. Hahn, "High-power and high-efficiency InGaN-based light emitters," *IEEE Trans. Electron Devices*, vol. 57, no. 1, pp. 79–87, Jan. 2010.

[15] I. Neokosmidis, T. Kamalakis, J. W. Walewski, B. Inan, and T. Sphicopoulos, "Impact of nonlinear LED transfer function on discrete multitone modulation: Analytical approach," *J. Lightw. Technol.*, vol. 27, no. 22, pp. 4970–4978, Nov. 15, 2009.

[16] T. Kamalakis, J. W. Walewski, G. Ntogari, and G. Mileounis, "Empirical volterra-series modeling of commercial light-emitting diodes," *J. Lightw. Technol.*, vol. 29, no. 14, pp. 2146–2155, Jul. 15, 2011.

[17] A. Alexeev, J.-P. M. Linnartz, K. Arulandu, and X. Deng, "Characterization of dynamic distortion in LED light output for optical wireless communications," *Photon. Res.*, vol. 9, no. 6, pp. 916–928, 2021.

[18] X. Deng et al., "Mitigating LED nonlinearity to enhance visible light communications," *IEEE Trans. Commun.*, vol. 66, no. 11, pp. 5593–5607, Nov. 2018.

[19] S. Mardanikorani, X. Deng, J.-P. M. Linnartz, and A. Khalid, "Compensating dynamic nonlinearities in LED photon emission to enhance optical wireless communication," *IEEE Trans. Veh. Technol.*, vol. 70, no. 2, pp. 1317–1331, Feb. 2021.

[20] G. Ghione, *Semiconductor Devices for High-Speed Optoelectronics*, vol. 116. Cambridge, U.K.: Cambridge Univ. Press, 2009.

[21] H. Chun, C.-J. Chiang, A. Monkman, and D. O'Brien, "A study of illumination and communication using organic light emitting diodes," *J. Lightw. Technol.*, vol. 31, no. 22, pp. 3511–3517, Nov. 15, 2013.

[22] Z.-Y. Wu, X.-Y. Liu, J.-S. Wang, and J. Wang, "Modulation index dependence of intensity modulation bandwidth in visible light communications," *Opt. Lett.*, vol. 43, no. 19, pp. 4570–4573, 2018.

[23] M. E. Raypah, B. K. Sodipo, M. Devarajan, and F. Sulaiman, "Estimation of optical power and heat-dissipation factor of low-power SMD LED as a function of injection current and ambient temperature," *IEEE Trans. Electron Devices*, vol. 63, no. 1, pp. 408–413, Jan. 2016.

[24] R. L. Boylestad and L. Nashelsky, *Electronic Devices and Circuit Theory*. Harlow, U.K.: Pearson Educ. 2009.

[25] X. Li, Z. Ghassemlooy, S. Zvanovec, M. Zhang, and A. Burton, "Equivalent circuit model of high power LEDs for VLC systems," in *Proc. 2nd West Asian Colloq. Opt. Wireless Commun. (WACOWC)*, 2019, pp. 90–95.

[26] P. Santhanam, D. J. Gray Jr., and R. J. Ram, "Thermoelectrically pumped light-emitting diodes operating above unity efficiency," *Phys. Rev. Lett.*, vol. 108, no. 9, 2012, Art. no. 097403.

[27] S. Karpov, "ABC-model for interpretation of internal quantum efficiency and its droop in III-nitride LEDs: A review," *Opt. Quantum Electron.*, vol. 47, no. 6, pp. 1293–1303, 2015.

[28] H. P. T. Nguyen et al., "Controlling electron overflow in phosphor-free InGaN/GaN nanowire white light-emitting diodes," *Nano Lett.*, vol. 12, no. 3, pp. 1317–1323, 2012.

[29] X. Deng, Y. Wu, A. Khalid, X. Long, and J.-P. M. Linnartz, "LED power consumption in joint illumination and communication system," *Opt. Exp.*, vol. 25, no. 16, pp. 18990–19003, 2017.

[30] M. Steer, *Microwave and RF Design*. Raleigh, NC, USA: NC State Univ., 2019.

[31] "OSRAM OSRAM OSTaR® projection compact, LE RTB N7WM multi color." LEDs-osram.com. Accessed: Jan. 25, 2024. [Online]. Available: https://ams-osram.com/products/multi-chips/multi-color-leds/osram-osram-ostar-projection-compact-le-rtb-n7wm

[32] Y. Wang, X. Chen, and Y. Xu, "Transmitter for 1.9 Gbps phosphor white light visible light communication without a blue filter based on OOK-NRZ modulation," *Opt. Exp.*, vol. 31, no. 5, pp. 7933–7946, 2023.

[33] P. A. Haigh et al., "A multi-CAP visible-light communications system with 4.85-b/s/hz spectral efficiency," *IEEE J. Sel. Areas Commun.*, vol. 33, no. 9, pp. 1771–1779, Sep. 2015.

[34] A. Gupta, N. Sharma, P. Garg, and M.-S. Alouini, "Cascaded FSO-VLC communication system," *IEEE Wireless Commun. Lett.*, vol. 6, no. 6, pp. 810–813, Dec. 2017.

[35] R. Mesleh, H. Elgala, and H. Haas, "Optical spatial modulation," *J. Opt. Commun. Netw.*, vol. 3, no. 3, pp. 234–244, 2011.